For the data analysis method used in this type of animal experiment to investigate synergism, Kelly and Rice (1990) proposed a method to evaluate the dose–response curve by smoothing method. Gennings and Carter (1995) and Gennings *et al.* (1997), on the other hand, proposed a method to evaluate synergism by using a model in which the response becomes flattened when there is no synergism. Using a similar plan to that of Gennings *et al.* (1997), Matsunaga *et al.* (2003) proposed a method to evaluate the difference in the responses with simultaneous administration of two substances from those estimated by applying an additive model to the data of single administration of each substance. They applied their proposed method to the actual data analysis. Other data analysis methods are also cited in Laska and Meisner (1989) and Machado and Robinson (1994).

For the experimental design evaluating the synergism, Hasegawa *et al.* (1996) proposed the experimental design of animal experiment for five or ten chemical mixture, and Straetemans *et al.* (2005) investigated a fixed-ratio design on *in vitro* study. Abdelbasit and Plackett (1982) and Tan *et al.* (2003) are also related to this issue. However, the situation of these researches differs from our case study. Our interest is limited to simply checking whether the effects of the chemicals are additive or not. And in the animal experiments, some assumptions and limitations are generated for the applicable information and experimental conditions.

In this kind of research, we thought that the problem of the experimental design is to determine appropriate dose levels for simultaneous administration and to select the appropriate number of animals for allocation to the dose levels. However, in the past research, the research directly related to this problem by the animal experiment was not found. Accordingly, based on the analysis methods proposed by Matsunaga *et al.* (2003), we investigated what type of design would be appropriate.

The paper is organized as follows. Section 2 introduces the conditions in the case study that motivated this paper, while Section 3 formulates the issues. Section 4 derived the appropriate design corresponding to the case studies dealt with this paper. Finally, Section 5 provides Conclusions and Discussions for future issues.

2. MOTIVATING CASE

According to the World Health Organization, an endocrine disruptor is defined as "an exogenous substance or mixture that alters function(s) of the endocrine system and causes adverse health effects in an intact organism, or its progeny or (sub)populations."

The effect of endocrine disruptors is not stimulated directly at the site of the adverse effect, but is mediated by the signal and occurs through nuclear receptor. Furthermore, there is more than one signal transduction system in humans and animals. Because nuclear receptors and transcription factors are redundant, there may be an interaction between different pathways, which leads to possible synergistic endocrine disruption action. Here the definition of "synergistic" is that if two chemicals produce the same endpoint, they bring about a larger response as compared to the anticipated response when these chemicals are purely added. Consequently, it is very important to realize the synergism between two endocrine disruptors such as "Genistein" and "bisphenol A (BPA)" through animal experiments for explaining the mechanism of action.

Both Genistein and BPA bind to estrogen receptors and elicit estrogenic responses to an organism including uterotrophic responses. Genistein is a phytoestrogen found relatively abundant in soybeans and its derivative foods. BPA is the basic monomer of polycarbonate plastic and epoxy resins widely used as a lining for food and beverage cans, in hard plastic baby and water bottles, toys, dental sealants, etc. It has been reported that BPA monomer can leached out to food and drinks especially when the

DOI: 10.1002/env

polymerization process is incomplete and/or the plastic is aged. These two estrogenic compounds can be found very commonly in our food environment. Therefore, it is of great importance from the point of the safety regulations to examine whether the combined effect is additive or synergistic.

For the experimental design of the research based on this background, some assumptions and limitations were generated for the applicable advanced information and experimental conditions. In the interests of simplicity, when explaining synergism research for two substances, the limitations are as follows.

First, before conducting the experiment that investigates synergism, advance knowledge can be obtained to some extent on dose–response curves for the single administration from preliminary experiments using each substance. Therefore, if the dose–response curve is nonlinear, by appropriate transformation of variables for the dose and response, it is possible to assume the dose–response curve to be approximately linear.

Second, the maximum dose of each substance used in the experiment is limited. We, for example, recognize in our experiments that the signal transduction system amplifies the signal at significantly smaller doses as compared to the dose used in normal toxicity studies. Other toxicities appear with higher doses, so that the endocrine disruption effect to be investigated is concealed. Because these maximum doses, $D_{A\max}$ and $D_{B\max}$, generally can be obtained through preliminary experiments, the range of dose levels used in the experiments can be limited.

Third, because various kinds of test substances are to be investigated, the number of animals, n, used in each experiment is relatively small. In our actual experience, the number of animals is approximately 40–50.

Fourth, the fundamental form of the experiment for investigating synergism is roughly decided. In an experiment using two substances A and B, we set single administration groups of G_{00} (at a dose level of 0), G_{A2}, and G_{B2} (at the maximum dose levels of $d_{A2} = D_{A\max}$ and $d_{B2} = D_{B\max}$, respectively), and groups G_{A1} and G_{B1} (at the middle dose levels of d_{A1} and d_{B1}, respectively), and administer the test substances after assigning the same number of animals n_s in every group. Independent of this, we set one or more simultaneous administration groups of G_{AB} with dose levels of the two substances at d_A and d_B. We measure responses by performing the experiment with this type of design, and estimate dose–response curves by forecasting synergism from the single administration group to confirm whether the response obtained in the simultaneous administration group is larger compared to that estimated.

Fifth, the observed response is usually quantitative variable such as the uterine weight of rats, which generally shows normal distribution, because it is difficult to define the additivity/synergism for the response in qualitative values.

Under the above conditions, what should be questioned for the design is what the most appropriate dose for simultaneous administration is, and whether to have more or less animals for the simultaneous administration group as compared to the single administration group. In order to obtain guidelines for these, this paper generalizes and formulates the above mentioned problems to make numerical evaluations under some conditions.

3. FORMULATION OF PROBLEM

3.1. Definition of synergism

In order to simplify the discussion, hereafter, we assume that there are two test substances denoted by A and B.

There have been many discussions in the past for how to define the terms additivity, synergism, and antagonism. Synergism is not defined unconditionally (Hewlett and Plackett, 1959; Berenberm, 1989).

Table 1. Difference between factorial design and triangular design

	Dose of A		
Dose of B	d_{A0}	d_{A1}	d_{A2}
(a) Factorial design			
d_{B0}	(1)	(2)	(3)
d_{B1}	(4)	(6)	(7)
d_{B2}	(5)	(8)	(9)
(b) Triangular design			
d_{B0}	(1)	(2)	(3)
d_{B1}	(4)	(6)	
d_{B2}	(5)		

Single chemical is administered at (1)–(5), whereas combination of two chemicals is administered at (6)–(9).

In fact, in the general remarks of these studies, many ideas are introduced for discussing synergism such as "independent joint action," "potentiation," "simple similar action," "complex action," and "dissimilar action." We will first explain the definition of synergism that is adopted in this paper.

From the standard statistical viewpoint, the dosages set certain dose level for the respective two substances as shown in Table 1(a). If the response at the simultaneous dose level is the sum of the effects generated by single substances, then the effect is considered to be additive. On the other hand, if it is large, there is a positive interaction and the effect is synergistic.

However, with toxic responses like endocrine disruption action, this point of view is not appropriate. Because, for this toxic response, as pointed out by, for example, Hasegawa *et al.* (1996), it is impossible to establish response linearity at doses that exceed the maximum dose for the respective substances, and thus it is impossible to determine whether a positive interaction is attributable to synergism or nonlinearity. Therefore, the following definition that expresses the tenets of Hewlett and Plackett (1959) by isobologram is adopted in this paper.

Label the expected response at dose d_A and d_B (doses for A and B) as $f(d_A, d_B)$. Also, label the single administration dose of A that results in an arbitrary response E as D_A, so that $f(D_A, 0) = E$. Similarly, label the dose of substance B that has expectation E as D_B. In the cases that motivated this study, A and B generate their responses in a similar stimulation process, the expected effects are proportional to the doses of A and B, and the effects of the two substances are additive. If these conditions hold, then $f(d_A, d_B) = E$ whenever (d_A, d_B) satisfies Equation (1).

$$\frac{d_A}{D_A} + \frac{d_B}{D_B} = 1 \tag{1}$$

The reason is that because a combination of dose levels like this represents simultaneous administration of A and B at an arbitrary ratio, using the amount that brings about a response of the same magnitude. If a response of magnitude E is consequently generated as expected, there is no special combined effect between the two chemicals. In this paper, when this relationship holds, the effect of the two substances is additive, or the two substances satisfy additivity.

On the other hand, if the two substances generate a synergistic response in different stimulation processes, it is considered that $f(d_A, d_B) > E$ is established with respect to an arbitrary (d_A, d_B) that satisfies Equation (1). In this paper, when this relationship is established, the two substances are synergistic, or satisfy synergism.

DOI: 10.1002/env

3.2. *Terminology, notation, and assumption*

The two-dimensional plane by plotting d_A (dose of A) on the x-axis and d_B (dose of B) on the y-axis is referred to as the dose plane, and the three-dimensional space by plotting the response on the z-axis above the dose plane is referred to as the response space.

In the experiment, the response is measured for each individual animal. The response that is measured is called the response variable, and is generally expressed by the symbol Z. The response variable Z measured for each individual is set as a random variable that follows a normal distribution independent of other individuals. Since it is assumed that the endpoint is organ weight as a target for application in the case study, such as endocrine disruptor study, it is considered that the assumption of the normal distribution is empirically valid. When the dose of the two substances administered is (d_A, d_B), the expected value is $E\{Z\} = f(d_A, d_B)$.

For single administration, that is, when the dose of one test substance is 0, Equation (2) can be assumed concerning the dose–response curve f.

$$f(d_A, 0) = \beta_0 + d_A\beta_A,\ f(0, d_B) = \beta_0 + d_B\beta_B \tag{2}$$

This assumes the dose–response curve for single administration to be linear. With this assumption, $f(d_A, d_B)$ is expressed by Equation (3). The two substances are additive if the hypothesis H_0 of Equation (4) holds, while synergistic if the hypothesis H_1 holds.

$$f(d_A, d_B) = \beta_0 + d_A\beta_A + d_B\beta_B + \Delta(d_A, d_B) \tag{3}$$

$$H_0 : \Delta(d_A, d_B) = 0,\ H_1 : \Delta(d_A, d_B) > 0 \text{ for all } (d_A, d_B) \tag{4}$$

The value of the dose used in the experiment is called the dose level, the collection of animals allocated for the dose level is called a group, and the number of animals for each group is called the group size, and the dose level of the group on the dose plane is called the group point. With this terminology, it is defined that "design is the set of group point and group size."

For numerical evaluation described in the next section, five groups of group size n_s for single administration and one group of group size n_m for simultaneous administration as described in Table 1(b) are assumed as the design. For the single administration group, the group points are set to be $(0, 0)$, $(d_{A1}, 0)$, $(d_{A2}, 0)$, $(0, d_{B1})$, $(0, d_{B2})$, and the response variables are distributed as normal with variance σ_s^2. For the simultaneous group, the group point is set to be (d_A, d_B), and the response variable is distributed as normal with variance σ_m^2

Let the sample mean of response variable in each group be Z_{00}, Z_{A1}, Z_{A2}, Z_{B1}, Z_{B2}, and Z_{AB}, respectively. It is assumed that $Z_{00}, \ldots, Z_{B2}$ are distributed as normal with the mean of Equation (2) and the variance σ_s^2/n_s, while Z_{AB} is distributed as normal with the mean of Equation (3) and the variance σ_m^2/n_m.

3.3. *Criterion for the appropriate design*

As criterion for the most appropriate design, it is natural to use the power in the hypothesis test of "H_0 versus H_1." Because the model is a linear model and the hypothesis is a linear hypothesis, a one-sided

t-test (or Welch test) with Equation (5) is naturally set as the test statistic.

$$T = \frac{\hat{\Delta}}{\sqrt{\hat{V}(\hat{\Delta})}} \tag{5}$$

Here, $\hat{\Delta}$ is the least square estimator of Δ, and the denominator of the statistics is the square root of the variance estimator.

The critical value of this test statistics is $t(\nu, \alpha)$, the upper 100α percentile of the t-distribution with degree of freedom ν, and the test is a one-sided test. In other words, A and B are judged to be synergistic when $T > t(\nu, \alpha)$.

This test, in short, detects the synergism when there is a statistically significant difference between Z_{AB} and the estimate obtained from the single administration groups assuming the dose–response surface under H_0.

4. EXAMPLES OF RECOMMENDED DESIGN

4.1. Real examples motivated the problem

We conducted many experiments and selected endocrine disruptor study as case study. This study was performed using triangular design such as Table 1(b). This design consisted of seven dose groups which included five group points for single administration and two group points for simultaneous administration. The endpoint was uterine weight gain and the main purpose was to evaluate whether the combined effect was synergistic or not. In order to explain the characteristic of the data, we took up two real examples. The details of these data are as follows.

Example 1. *Chemical A: genistein (mg/kg), chemical B: BPA (mg/kg)*

1. Group points for the single administration: $(d_A, d_B) = (0, 0), (12.5, 0), (25, 0), (0, 35), (0, 70)$.
2. Group points for simultaneous administration: $(d_A, d_B) = (6.25, 17.5), (12.5, 35)$.
3. Group size: $n_s = 6, n_m = 6, n = 42$.
4. Mean $\pm$ standard deviation of observed values

$$(d_A, d_B) = (0, 0) : 84.0 \pm 7.1$$
$$(d_A, d_B) = (12.5, 0) : 111.2 \pm 9.3, \quad (d_A, d_B) = (25, 0) : 149.5 \pm 33.7$$
$$(d_A, d_B) = (0, 35) : 138.4 \pm 16.2, \quad (d_A, d_B) = (0, 70) : 181.0 \pm 24.4$$
$$(d_A, d_B) = (6.25, 17.5) : 141.1 \pm 11.4, \quad (d_A, d_B) = (12.5, 35) : 180.2 \pm 26.8$$

5. Estimated value of Δ: 15.6.
6. Result of t-test: Significant in one-sided Welch test with significance level 2.5% $T = 2.19$, $\nu = 19$, $p = 0.02$.

Example 2. *Chemical A: diethylstilbestrol (μg/kg), chemical B: genistein (mg/kg)*

1. Group points for the single administration: $(d_A, d_B) = (0, 0), (0.1, 0), (0.2, 0), (0, 12.5), (0, 25)$.
2. Group points for simultaneous administration: $(d_A, d_B) = (0.05, 6.25), (0.1, 12.5)$.

3. Group size: $n_s = 6, n_m = 6, n = 42$.
4. Mean $\pm$ standard deviation of observed values

$$(d_A, d_B) = (0, 0) : 91.2 \pm 16.2$$
$$(d_A, d_B) = (0.1, 0) : 92.3 \pm 9.7, \quad (d_A, d_B) = (0.2, 0) : 96.5 \pm 5.4$$
$$(d_A, d_B) = (0, 12.5) : 165.4 \pm 27.0, \quad (d_A, d_B) = (0, 25) : 220.8 \pm 27.5$$
$$(d_A, d_B) = (0.05, 6.25) : 141.8 \pm 12.8, \quad (d_A, d_B) = (0.1, 12.5) : 183.5 \pm 10.3$$

5. Estimated value of Δ: 19.5.
6. Result of t-test: significant in one-sided Welch test with significance level 2.5% $T = 3.98$, $\nu = 31$, $p < 0.01$.

From the above results, we suggested that the combinations for these two agents were synergistic. The synergism was observed in the real situations such as endocrine disruptor study.

4.2. Recommended group point selection

The example introduced in the preceding section has two simultaneous administration groups. In this section, we investigate the most appropriate dose level among several dose levels in the case of one simultaneous administration group. The conditions in the investigation are as follows. The conditions are set pursuant to the example in the preceding section except for assuming $\sigma = 1$ without losing any generality.

4.2.1. Fixed condition.

1. Group points for single administration: $(d_A, d_B) = (0, 0), (1, 0), (2, 0), (0, 1), (0, 2)$.
2. Group size: $n_s = 6, n_m = 12$.
3. Parameters in the dose–response curve: $\beta_0 = 1.0, \beta_A = 1.0, \beta_B = 1.0$.
4. Variance σ^2: $\sigma_s^2 = \sigma_m^2 = 1.0$.
5. Nominal significance level of t-test: one-sided 2.5%.

4.2.2. Varied condition.

6. Group points for simultaneous administration: $d_A = 0.1(0.1)2.0, d_B = 0.1(0.1)2.0$.
7. Strength of synergism Δ:
   Case 1 (constant case): $\Delta = 1.0$
   Case 2 (square root case): $\Delta = 0.8\sqrt{(d_A + d_B)}$
   Case 3 (linear case): $\Delta = 0.6(d_A + d_B)$

Numerical calculations were performed to calculate the power under the above conditions. The left-hand side of Figures 1–3 shows a three-dimensional display on the vertical axis above the dose plane of the power in Cases 1–3, respectively. On the other hand, the right-hand side of Figures 1–3 represents power functions when $d_A = d_B$ at the dose level for simultaneous administration group.

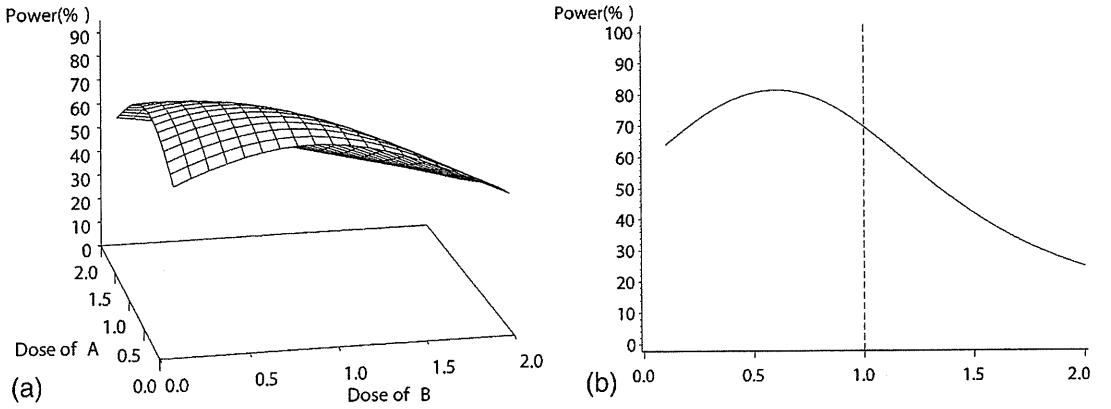

Figure 1. Power surface on the (a) dose plane and power function on the (b) dose for a simultaneous administration group with a constant surplus case (Case 1)

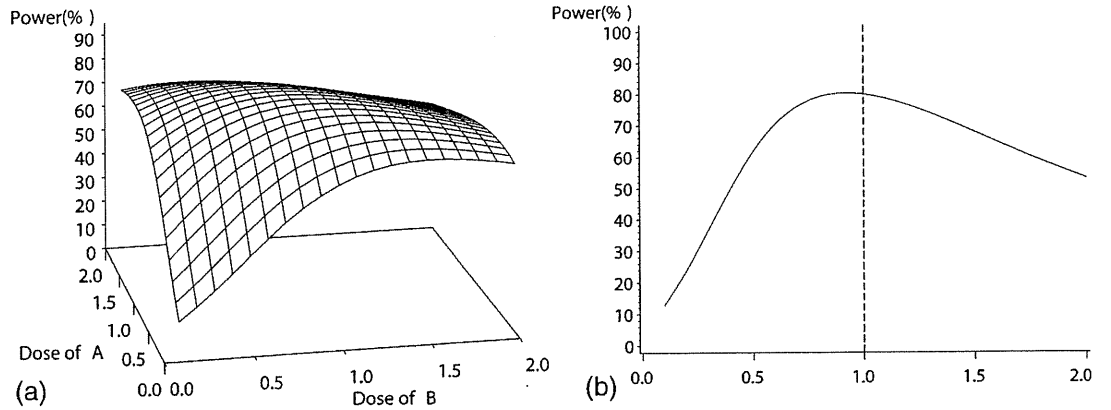

Figure 2. Power surface on the (a) dose plane and power function on the (b) dose for a simultaneous administration group with a square root surplus case (Case 2)

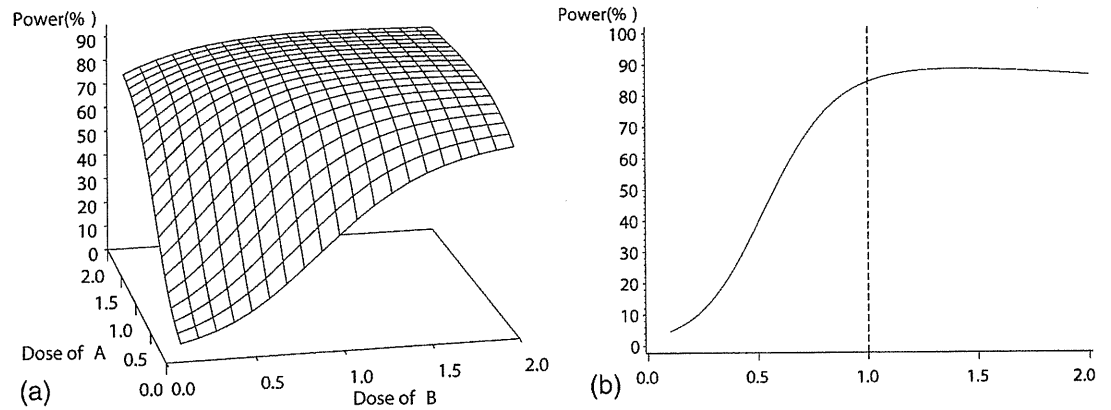

Figure 3. Power surface on the (a) dose plane and power function on the (b) dose for a simultaneous administration group with a linear surplus case (Case 3)

DOI: 10.1002/env

According to Figure 1, the power is high when the group point of the simultaneous administration group is within the triangular region and the power is low when it is located outside that region. Consequently, the design to evaluate synergism should have the group point within the triangle region. Figure 2 shows the power reaches a peak near the boundary of the triangular region and decreases apart from the triangular region as the dose increases. In consequence, the group point should be located on the boundary of triangle region. Finally, according to Figure 3, the power achieves the steady state on the boundary of the triangular region and reaches a peak slightly outside the triangular region when Δ becomes larger linearly as the dose increases. In numerical example, recommended group point in Cases 1–3 is, respectively, $(d_A, d_B) = (0.6, 0.6)$, $(0.9, 0.9)$, $(1.4, 1.4)$ and the power is 81.4%, 80.4%, 88.4%, respectively.

The sensitivity analysis was conducted to investigate the usefulness of location of the group point in the real study, such as two group points $(d_A, d_B) = (0.5, 0.5)$ and $(1.0, 1.0)$. In this section, only group points for simultaneous administration were changed in the following way and all other conditions were the same.

4.2.3. Group points for simultaneous administration.

(1) $(d_A, d_B) = (0.6, 0.6)$ (recommended in Case 1)
(2) $(d_A, d_B) = (0.9, 0.9)$ (recommended in Case 2)
(3) $(d_A, d_B) = (1.4, 1.4)$ (recommended in Case 3)
(4) $(d_A, d_B) = (1.0, 1.0)$ (on the boundary)
(5) $(d_A, d_B) = (0.5, 0.5), (1.0, 1.0)$ (real study)

Here, the total sample size for simultaneous administration groups is fixed in all group points (1)–(5). Then n_m for two groups' simultaneous design such as (5) is half of that for one group's design.

The numerical calculation was conducted under the above conditions. Table 2 summarizes the reduction of power from a recommended group point. When the group point is located close to the boundary of the triangular region, the reductions of power from a recommended group point are small. Furthermore, in the situation of real studies, the loss of power is negligible compared to that in a recommended group point. It is considered that the configuration of the group points in real study is reasonable from the statistical viewpoint.

4.3. Recommended group size

In this section, under conditions in which the total number of animals is fixed and the effect sizes are varied, we investigate the group size of the simultaneous administration group that maximizes the power.

Table 2. Reduction of power from a recommended group point in three cases

Group point (d_A, d_B)	Case 1 (constant case)	Case 2 (square root case)	Case 3 (linear case)
(0.6, 0.6)	0.0	−10.2	−34.7
(0.9, 0,9)	−7.3	0.0	−9.3
(1.4, 1.4)	−34.6	−9.7	0.0
(1.0, 1.0)	−12.2	−0.4	−5.1
(0.5, 0.5), (1.0, 1.0)	−2.0	−2.6	−19.7

n_m for two group points is half of that for one group.

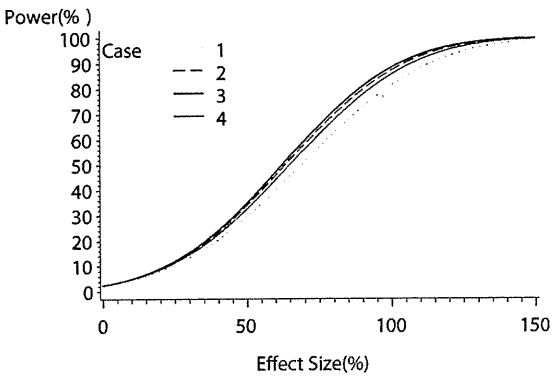

Figure 4. Relation between power and group size in four cases

4.3.1. Fixed conditions.

1. Group points for single administration: $(d_A, d_B) = (0, 0), (1, 0), (2, 0), (0, 1), (0, 2)$.
2. Group point for simultaneous administration: $(d_A, d_B) = (0.6, 0.6)$.
3. Parameters in the dose–response curve: $\beta_0 = 1.0$, $\beta_A = 1.0$, $\beta_B = 1.0$.
4. Variance σ^2: $\sigma_s^2 = \sigma_m^2 = 1.0$.
5. Nominal significance level of t-test: one-sided 2.5%.
6. Total number of animals: $n = 42$.

4.3.2. Varied conditions.

7. Group size:
   Case 1: $n_s = 6, n_m = 12$
   Case 2: $n_s = 5, n_m = 17$
   Case 3: $n_s = 4, n_m = 22$
   Case 4: $n_s = 3, n_m = 27$
8. Effect Size: $\Delta/\sigma_m = 0.1(0.1)1.5$.

Figure 4 shows the results of the numerical calculations, with the power on the vertical axis and the effect size on the horizontal axis. According to Figure 4, regardless of the effect size, Case 3 gives the maximum power. Because the group size is constrained to be an integer, it is not possible to give the most appropriate group size as a continuous value. The power becomes larger when the group size of the simultaneous administration group is set larger than that of the single administration group. When $n = 42$, what is prominent is the fact that the group size of 22 in the simultaneous administration group is nearly equal to the total number of animals in the single administration group, $4 \times 5 = 20$.

5. DISCUSSION

5.1. Conclusion under assumed conditions

In the previous section, we investigated applicable designs assuming that the response variables follow a homoscedastic normal distribution, that the dose–response relationship for single administration is

linear, that synergism is defined as a larger response obtained with simultaneous administration as compared to the dose plane obtained with single administration by assuming additivity, that there are five groups for single administration and one group for simultaneous administration, etc.

As the results of numerical calculation for the group point, when the departure Δ from additivity is proportional to square root of the dose, it is revealed that the group point for the simultaneous administration group should be on the boundary of the triangle region. Here, the results seemed to be reasonable. Because it is natural to expect that the departure Δ does not continue to increase along with the dose constantly. So, we applied these two situations as the sensitivity analysis. When the departure Δ become larger linearly along with the dose, the group point should be located slightly outside the triangle region. On the other hand, the group point should be set inside the triangle region when the departure Δ is constant. However, the group point should be placed on the boundary of the triangular region, because the reduction of power from a recommended group point is small. This means that the conventional design in the real study is appropriate.

Subsequently, with respect to the group size, we revealed that the total number of animals allocated to the simultaneous administration group should be same size as that in the single administration group.

5.2. *Heteroscedasticity*

When heteroscedasticity in data is expected from the past research, it is required to adjust the degree of freedom by using the Welch test. For the cases discussed in this paper, we used the Welch test, which is robust for heteroscedasticity because there is a tendency in real data for the variance to increase with an increase in responses although the number of animals is small. However, the Welch test does not control a type 1 error below the nominal significance level under heteroscedasticity. It is, therefore, required to confirm, *ex post facto*, the type 1 error when the degree of heteroscedasticity is large.

5.3. *Linearity*

For the cases discussed in this paper, based on advanced information, it was possible to select the dose so that there is linearity with the single administration group. This was easier due to the fact that the number of dose levels in the single administration group was small (three levels). From the experimental results, it was also confirmed that the linearity assumptions were established to some extent. When using the results in this paper, it is important to confirm the dose–response relationship in preliminary experiments or in past experiments using analogous substances. It is necessary to examine, *ex post facto*, the linearity by displaying in figure or by linearity tests.

5.4. *Group size*

The group size must be an integer of at least 1. In addition, the total number of animals must be a comparatively small. Under these conditions, as in this paper, it is necessary to obtain the appropriate design using numerical calculations, separately considering a combination of possible group sizes. However, in order to generalize these results, it is useful to perform power calculations, taking the group size as a continuous value. When calculating the recommended ratio of the total number of animals in the single administration group to the group size of the simultaneous administration group, the results shown in Figure 5 are obtained.

When determining the appropriate group point of the simultaneous administration group, with the departure Δ from the additivity being constant, the highest power is obtained by setting the number of

DOI: 10.1002/env

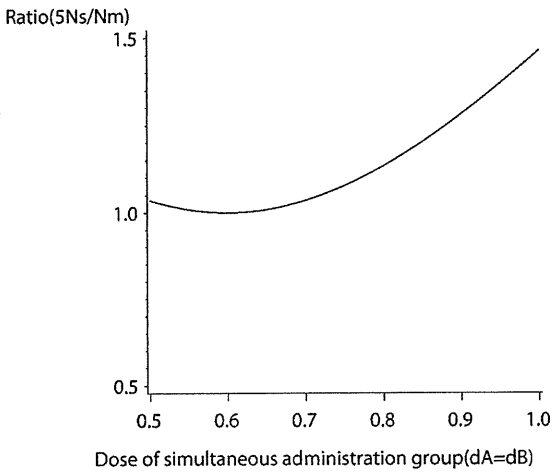

Figure 5. Recommended ratio of the group size between single administration group and simultaneous administration group

animals at a ratio of 1:1 between the single administration group and the simultaneous administration group.

When determining the simultaneous administration group on the boundary of the triangular region, a theoretical calculation shows that the allocation at a ratio of 1.464:1 is appropriate. In other words, it is best to set the total number of animals in the single administration group to be approximately 1.5 times the total number of animals in the simultaneous administration group. The reason is that because it is theoretically favorable for the accuracy of estimates based on additivity to be equal to that based on simultaneous administration.

5.5. Practical consideration on the recommended design

In the numerical examples of the previous section, we showed that the group point for the simultaneous administration on the boundary of the triangular region is not necessarily best and the recommended number of animals for the simultaneous administration group is considerably greater than those for single administration groups.

Although these results speciously imply that the design exemplified in the Subsection 4.1 should be replaced with the recommended design shown in this paper in future, we think it is not always true, because we have to take practical conditions into consideration, which were not incorporated in the assumptions to derive the recommended design.

One of them is the robustness or stability of the result of data analysis in such experiments. The situation is quite similar to that for the recommended design at linear regression analysis, for example, related to a single chemical experiment. Actually, if we can entirely assume the linearity of the dose–response relationship in regression analysis, the recommended design is to allocate a half of animals to the maximum dose and the remaining half to the minimum dose, while such design is really not adopted and animals are evenly allocated to uniformly distributed three or four doses probably to secure the robustness of the result of data analysis. Likewise, when the functional relationship of the Δ is not particularly clear, or when there is concern for the instability in squeezing the simultaneous administration group into one group in our experiments, the design with two or three simultaneous

administration groups within the triangular region must be practical. Since the mathematical formulation in such condition could not be established up to present due to its difficult nature, we left it for future investigation.

5.6. *Other issues for future investigation*

When the number of test substances is 3 or more, there needs to be strict controls for the number of required animals. Therefore, a design must be determined by examining the design conditions in detail for each case. Under this condition, an investigation following the same approach as in this paper is necessary. This is another problem to be addressed in future research.

In this paper, we introduced a test statistic by using the unweighted least squares method. The weighted least squares method must be considered when the rules for the size of variance are understood from past research, such that variance linearly becomes larger along with the dose. The specific design in this instance is also to be investigated in the future.

ACKNOWLEDGMENT

We thank Professor Takashi Sozu at Osaka University for his assistance in the preparation of this paper. We are grateful to the Editor-in-Chief and two anonymous reviewers for their comments that greatly improved this paper.

REFERENCES

Abdelbasit KM, Plackett RL. 1982. Experimental design for joint action. *Biometrics* **38**: 171–179.
Berenbaum MC. 1989. What is synergy? *Pharmacological Review* **41**: 93–141.
Gennings C, Schwartz P, Carter WH, Simmons JE. 1997. Detection of departures from additivity in mixtures of many chemicals with a threshold model. *Journal of Agricultural, Biological, and Environmental Statistics* **2**: 198–211.
Gennings C, Carter WH. 1995. Utilizing concentration-response data from individual components to detect statistically significant departures from additivity in chemical mixture. *Biometrics* **51**: 1264–1277.
Hasegawa R, Yoshimura I, Imaida K, Ito N, Shirai T. 1996. Analysis of synergism in hepatocarcinogenesis based on preneoplastic foci induction by 10 heterocyclic amines in the rat. *Japanese Journal of Cancer Research* **87**: 1125–1133.
Hewlett PS, Plackett RL. 1959. A unified theory for quantal response to mixtures of drugs: noninteractive action. *Biometrics* **15**: 591–610.
Kanno J, Onyon L, Haseman J, Fenner-Crisp P, Axhby J, Owens W. 2001. The OECD program to validate the rat uterotrophic bioassay to screen compounds for *in vivo* estrogenic response: phase 1. *Environmental Health Perspectives* **109**: 785–794.
Kelly C, Rice J. 1990. Monotone smoothing with application to dose-response curve and the assessment of synergism. *Biometrics* **46**: 1071–1085.
Laska EM, Meisner MJ. 1989. Testing whether an identified treatment is best. *Biometrics* **45**: 1139–1151.
Matsunaga N, Kanno J, Yoshimura I. 2003. A statistical method for judging synergism application to an endocrine disruptor animal experiment. *Environmetrics* **14**: 213–222.
Machado SG, Robinson GA. 1994. A direct, general approach based on isobologram for assessing the joint action of drugs in pre-clinical experiment. *Statistics in Medicine* **13**: 2289–2309.
Roy P, Esteve J. 1998. Using relative risk models for estimating synergy between two risk factors. *Statistics in Medicine* **17**: 1357–1373.
Straetemans R, O'Brien T, Wouters L, Dun JV, Janicot M, Bijnens L, Burzykowski T, Aerts M. 2005. Design and analysis of drug combination experiments. *Biometrical Journal* **47**: 299–308.
Tan M, Fang HB, Tian GL, Houghton PJ. 2003. Experimental design and sample size determination for testing synergism in drug combination studies based on uniform measures. *Statistics in Medicine* **22**: 2091–2100.

Neonatal Exposure to Low-Dose 2,3,7,8-Tetrachlorodibenzo-*p*-Dioxin Causes Autoimmunity Due to the Disruption of T Cell Tolerance[1]

Naozumi Ishimaru,* Atsuya Takagi,† Masayuki Kohashi,* Akiko Yamada,* Rieko Arakaki,* Jun Kanno,† and Yoshio Hayashi[2]*

Although 2,3,7,8-tetrachlorodibenzo-*p*-dioxin (TCDD) has been shown to influence immune responses, the effects of low-dose TCDD on the development of autoimmunity are unclear. In this study, using NFS/*sld* mice as a model for human Sjögren's syndrome, in which the lesions are induced by the thymectomy on day 3 after birth, the autoimmune lesions in the salivary glands, and in later phase, inflammatory cell infiltrations in the other organs were developed by neonatal exposure to nonapoptotic dosage of TCDD without thymectomy on day 3 after birth. We found disruption of thymic selection, but not thymic atrophy, in TCDD-administered mice. The endogenous expression of aryl hydrocarbon receptor in the neonatal thymus was significantly higher than that in the adult thymus, suggesting that the neonatal thymus may be much more sensitive to TCDD compared with the adult thymus. In addition, the production of T_H1 cytokines such as IL-2 and IFN-γ from splenic $CD4^+$ T cells and the autoantibodies relevant for Sjögren's syndrome in the sera from TCDD-exposed mice were significantly increased compared with those in control mice. These results suggest that TCDD/aryl hydrocarbon receptor signaling in the neonatal thymus plays an important role in the early thymic differentiation related to autoimmunity. *The Journal of Immunology,* 2009, 182: 6576–6586.

The toxicity of 2,3,7,8-tetrachlorodibenzo-*p*-dioxin (TCDD),[3] the environmental contaminant, has been shown to influence various biological responses such as immunological, reproductive, and neurobehavioral (1–3). It has been reported that TCDD induces thymic atrophy and suppresses a variety of T cell-dependent immune responses, including delayed-type and contact hypersensitivity responses and the activity of CTL itself (4–7). However, TCDD has been shown to enhance the proliferation and cytokine production of mitogen- or Ag-stimulated T cells (8). In this context, when a DO11.10 transgenic T cell model was used to investigate the effects of TCDD on the activation of Ag-specific $CD4^+$ T cells by transfer of $CD4^+$ T cells into TCDD-treated recipient mice, the exposure to TCDD had little effect on the initial activation, but on day 3 after OVA-peptide injection the T cell proliferation of TCDD-treated recipients was enhanced compared with that of control recipients (9). Thus, the effect of TCDD seems to be dependent on the developmental state and active state of the T cells. As for the effects of TCDD on B cells, it was reported that TCDD inhibited B cell proliferation triggered by LPS, surface Ig cross-linking, or PMA/ionomycin (10, 11). Moreover, the in vivo suppressive effect of TCDD on T cell-dependent Ab response to sheep RBC (SRBC) was found as an immunotoxicity of TCDD (12). However, the effects of TCDD on autoimmunity or on autoantibody production in autoimmune animal models have not been demonstrated.

A combination of immunologic, genetic, and environmental factors may play a key role on the development of autoimmune disease, which is induced by the breakdown of central or peripheral tolerance (13–15). Sjögren's syndrome (SS) is generally considered to be a T cell-mediated autoimmune disorder characterized by lymphocytic infiltrates and destruction of the exocrine glands, particularly of the salivary glands, and systemic production of autoantibodies against the ribonucleoprotein particles SS-A/Ro and SS-B/La (16–18). We have established and analyzed an animal model for SS in NFS/*sld* mutant mouse thymectomized 3 days after birth (3d-Tx) (19–21). It is well established that 3d-Tx in a certain strain of mice results in spontaneous development of inflammatory lesions similar to human autoimmune diseases in the thyroid, ovary, kidney, testis, and stomach, but little is known about the mechanisms leading to the induction of autoimmunity (22–25). From the findings in 3d-Tx autoimmune models, the initiation of autoreactivity is thought to be due to the retardation of regulatory T (Treg) cell differentiation together with lymphopenia caused by neonatal thymectomy. In other words, the impairment of T cell differentiation and/or maturation in the neonatal thymus may cause the initiation of T cell self-reactivity. Although the perinatal exposure to TCDD has been shown to induce the suppression of cell-mediated immunity to a more severe degree than those in adult exposure, the association of neonatal exposure to TCDD with the development of autoimmunity remains unclear (5, 6).

*Department of Oral Molecular Pathology, Institute of Health Biosciences, University of Tokushima Graduate School, Kuramotocho, Tokushima, Japan; and †Division of Cellular and Molecular Toxicology, Biological Safety Research Center, National Institute of Health Sciences, Kamiyoga, Setagayaku, Tokyo, Japan

Received for publication July 14, 2008. Accepted for publication March 17, 2009.

The costs of publication of this article were defrayed in part by the payment of page charges. This article must therefore be hereby marked *advertisement* in accordance with 18 U.S.C. Section 1734 solely to indicate this fact.

[1] This work was supported by a Health Sciences Research Grant (H17, 18, and 19-kagaku-ippan-003) from the Ministry of Health, Labor and Welfare, Japan and a Grant-in-Aid for Scientific Research (no. 17109016) from the Ministry of Education, Culture, Sports, Science and Technology of Japan.

[2] Address correspondence and reprint requests to Dr. Yoshio Hayashi, Department of Oral Molecular Pathology, Institute of Health Biosciences, University of Tokushima Graduate School, 3-18-15 Kuramotocho, Tokushima 770-8504, Japan. E-mail address: hayashi@dent.tokushima-u.ac.jp

[3] Abbreviations used in this paper: TCDD, 2,3,7,8-tetrachlorodibenzo-*p*-dioxin; 3d-Tx, thymectomized 3 days after birth; AhR, aryl hydrocarbon receptor; AIRE, autoimmune regulator; ARNT, AhR nuclear translocator; DN, double negative; DP, double positive; DRE, dioxin responsive element; IRF, IFN regulatory factor; SP, single positive; SS, Sjögren's syndrome; TEC, thymic epithelial cell; Treg, regulatory T; XRE, xenobiotic response element.

www.jimmunol.org/cgi/doi/10.4049/jimmunol.0802289

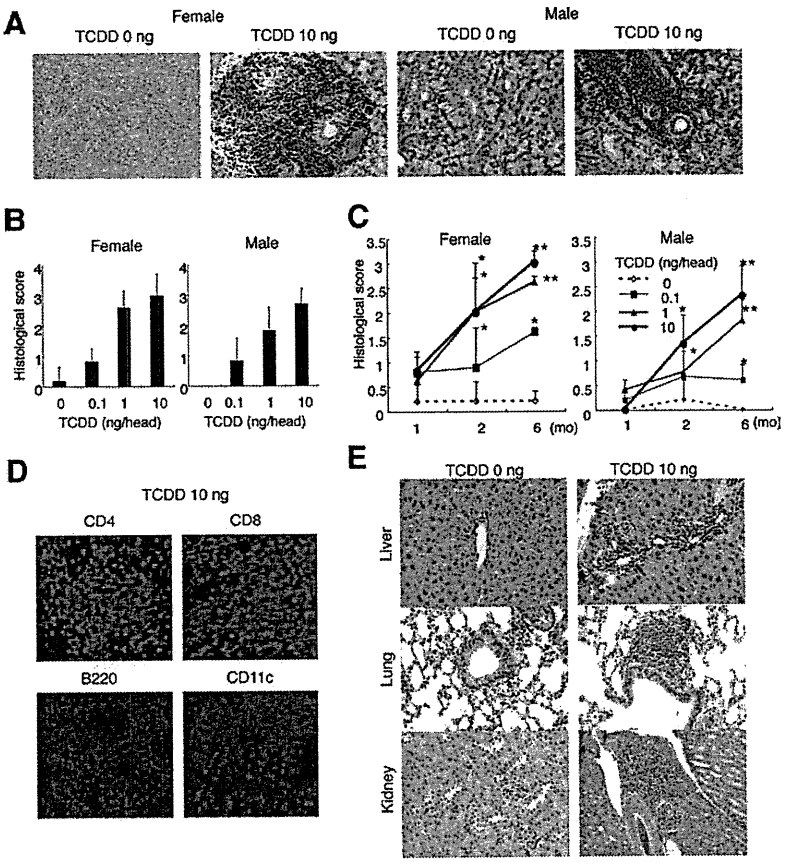

FIGURE 1. Inflammatory lesions induced by neonatal exposure to low-dose TCDD. *A*, Histology of salivary glands in female and male mice (6 mo) treated with 0 and 10 ng of TCDD were shown. H&E staining was performed using paraffin-embedded sections. Photos are representative of five to seven mice in each group. *B*, Histological score of the salivary glands at 6 mo of age was evaluated using the sections stained with H&E. Results are shown as the mean ± SD in the five to seven mice in each group. *C*, The change of inflammatory lesions from 1 to 6 mo of age in female and male mice treated with low-dose TCDD. Results are shown as the mean ± SD in the five to seven mice in each group. *, $p < 0.05$; **, $p < 0.005$. *D*, Immune cells in the inflammatory lesions of salivary glands from TCDD-treated mice at 6 mo of age were analyzed by immunofluorescence staining using anti-CD4, CD8, B220, and CD11c mAbs with Alexa Fluor 568-conjugated rat IgG (H+L) as the secondary Abs. Nuclei were stained with 4′,6-diamidino-2-phenylindole. Photos are representative of three to five sections in each group. *E*, Inflammatory lesions of liver, lung, and kidney induced by TCDD treatment. The sections from TCDD-treated mice at 6 mo of age were stained with H&E. Photos are representative of five to seven mice in each group.

One mechanism of TCDD action is binding and activation of the aryl hydrocarbon receptor (AhR) (1, 26). The AhR is a cytosolic transcription factor of the basic helix-loop-helix family. The activated receptor heterodimerizes with the AhR nuclear translocator (ARNT) in the nucleus and binds the xenobiotic response elements (XREs), also known as dioxin responsive elements (DREs), and alters the expressions of various genes such as cytochrome P450 1A1 (CYP1A1). TCDD, via the AhR, has been shown to have a variety of effects on T cell development and function, including decreasing the number of thymocytes by apoptosis and altering the effector functions of mature Th and T killer cells (27–30). Although a variety of studies have been performed to determine how high-dose TCDD is influencing T cells and the thymus (29–31), the mechanism and targets of its actions are still unclear. In addition, TCDD also induced the binding of several NF-κB proteins to a κB site, one of which overlapped with a DRE site (32). It has been uncertain whether the neonatal exposure to low-dose TCDD in vivo influences the TCDD signaling including AhR, CYP1A1, or NF-κB of immune cells.

In this study, we evaluated whether the immunotoxicity of nonapoptotic and low-dose TCDD during neonatal period influences the development of autoimmune disease in the murine SS-susceptible strain. Moreover, the correlation between the TCDD-induced signaling pathway in neonatal T cells and the initiation of self-reactivity in vivo was analyzed.

Materials and Methods

Mice

NFS/N strain carrying the mutant gene *sld* was reared in our specific pathogen-free mouse colony, and given food and water ad libitum. Experiments were humanely conducted under the regulation and permission of the Animal Care and Use Committee of the National Institute of Health Sciences, Tokyo, Japan and the University of Tokushima, Tokushima, Japan.

Neonatal administration of TCDD

Intraperitoneal injection of 10 μl of corn oil including TCDD (0, 0.1, 1, or 10 ng/mouse) with neonatal mice was performed on day 0, 1, and 2 after birth. Treatment of TCDD and TCDD-injected mice followed the rules of the National Institute of Health Sciences.

Histology

All organs were removed from the mice, fixed with 4% phosphate-buffered formaldehyde (pH 7.2), and prepared for histologic examination. Formalin-fixed tissue sections were subjected to H&E staining, and three pathologists independently evaluated the histology without being informed of the condition of each individual mouse. Histological changes were scored according to the method proposed by White and Casarett (33), as follows: 1 = 1–5 foci composed of >20 mononuclear cells per focus; 2 = >5 such foci, but without significant parenchymal destruction; 3 = degeneration of parenchymal tissue; 4 = extensive infiltration of the glands with mononuclear cells and extensive parenchymal destruction. Histological evaluation was performed in a blinded manner, and one tissue section from each salivary and lacrimal gland was examined.

Confocal microscopic analysis

Frozen sections were stained with 1 μg/ml primary Abs against CD4, CD8, B220, and CD11b/c (eBioscience) for 1 h. After three washes in PBS, the sections were stained with Alexa Fluor 568 donkey anti-rat IgG (H+L) (Molecular Probes) as the second Abs for 30 min and washed with PBS. The nuclei was stained with 4′,6-diamidino-2-phenylindole. The sections were visualized with a laser scanning confocal microscope (Carl Zeiss). A 63 × 1.4 oil differential interference contrast objective lens was used. Quick Operation Version 3.2 (Carl Zweiss) for imaging acquisition and Adobe Photoshop CS2 (Adobe System) for image processing was used.

Table I. *Incidence of inflammatory lesions in TCDD-treated mice*

	Female			Male		
	1 mo	2 mo	6 mo	1 mo	2 mo	6 mo
Liver treated with TCDD (ng)						
0	0/5 (0)	0/7 (0)	0/5 (0)	0/6 (0)	0/6 (0)	0/9 (0)
0.1	0/6 (0)	2/8 (25)	2/5 (40)	0/5 (0)	0/6 (0)	2/6 (33)
1	1/5 (20)	2/6 (33)	1/6 (17)	4/8 (50)	0/6 (0)	2/6 (33)
10	2/5 (40)	3/6 (50)	2/6 (33)	2/6 (33)	4/6 (67)	5/7 (71)
Lung treated with TCDD (ng)						
0	0/5 (0)	0/7 (0)	1/6 (17)	0/6 (0)	0/7 (0)	0/9 (0)
0.1	0/6 (0)	4/8 (50)	3/5 (60)	0/5 (0)	0/5 (0)	3/6 (50)
1	1/5 (20)	2/6 (33)	4/6 (67)	2/8 (25)	3/6 (50)	6/6 (100)
10	2/5 (40)	3/6 (50)	6/6 (100)	1/6 (17)	6/6 (100)	7/7 (100)
Kidney treated with TCDD (ng)						
0	0/5 (0)	0/7 (0)	0/6 (0)	0/6 (0)	0/7 (0)	0/9 (0)
0.1	0/6 (0)	0/8 (0)	1/5 (20)	1/5 (20)	3/5 (60)	4/6 (67)
1	0/5 (0)	0/6 (0)	2/6 (33)	2/8 (25)	4/6 (67)	5/6 (83)
10	1/5 (20)	3/6 (50)	2/6 (33)	2/6 (33)	6/6 (100)	5/7 (71)

The incidence of inflammatory lesions in the liver, lung, and kidney was histologically evaluated using the H&E-stained sections of the TCDD-treated NFS/*sld* mice at 1, 2, and 6 mo of age. The number of inflammatory lesion-induced mice in the organ/the total number of treated mice (%) is indicated.

Flow cytometric analysis

Surface markers were identified by mAbs with BD FACSCant flow cytometer (BD Biosciences). Rat mAbs to FITC-, PE-, or PE-Cy5-conjugated anti-B220, Thy1.2, CD4, CD8, CD25, and CD44 mAbs (eBioscience) were used. Intracellular Foxp3 expression was analyzed with an intracellular Foxp3 detection kit (eBioscience) according to the manufacturer's instructions. For intracellular AhR expression, cells were stained with PE-Cy5.5-conjugated anti-CD4, PE-conjugated anti-CD8, PE-Cy7-conjugated anti-CD44, allophycocyanin-conjugated anti-CD25 mAbs, and then fixed in fixation/permeabilization solution (eBioscience) for 18 h at 4°C. After washing twice with the permeabilization buffer (eBioscience), the cells were blocked with Fc block for 40 min on ice, and incubated in rabbit anti-AhR polyclonal Ab (BIOMOL) for 2 h at 4°C. After washing with the permeabilization buffer, the cells were stained with FITC-conjugated ant-rabbit IgG for 30 min at 4°C for flow cytometric analysis of multicolors. The data were analyzed with FlowJo FACS Analysis software (Tree Star).

Proliferation assay

Cell proliferation was evaluated by counting of divisions by CFSE (Molecular Probes) dilution of labeled cells. After stimulation by anti-CD3 and

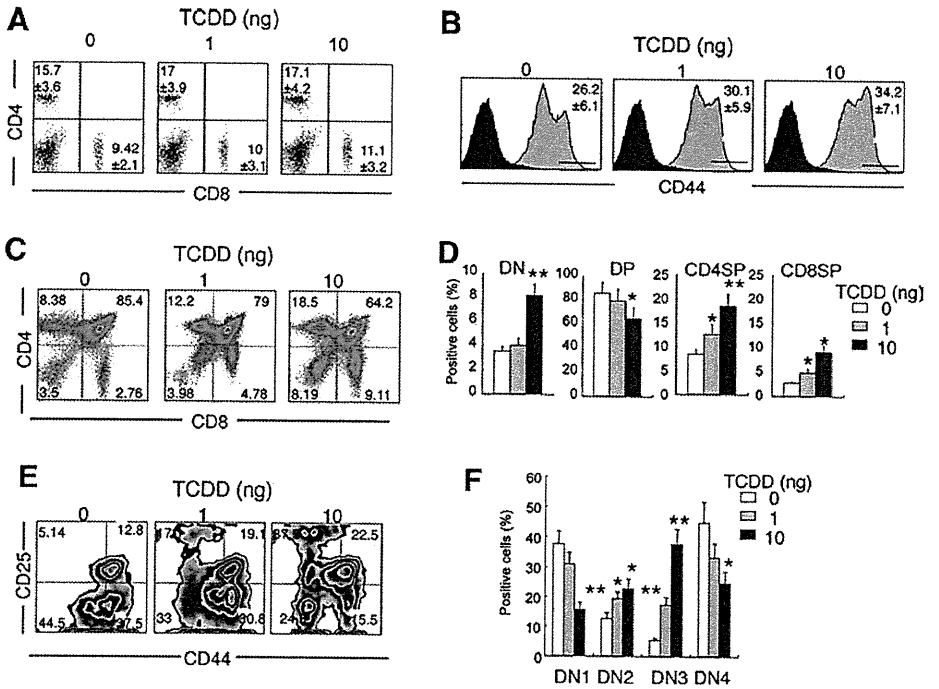

FIGURE 2. The effect of in vivo TCDD injection on T cell phenotypes. *A*, CD4 and CD8 expressions on spleen cells from female TCDD-treated mice at 6 mo of age were analyzed by flow cytometry. Positive cells (%) were indicated as the mean ± SD of five to seven mice in each group. *B*, CD44 expression on $CD4^+$ T cells in spleen from TCDD-treated mice. $CD44^{high}$ cells (%) are indicated as the mean ± SD of five to seven mice in each group. *C*, T cell differentiation in thymus of TCDD-treated mice was analyzed by flow cytometry using CD4 and CD8 expressions. Figures are representative of five to seven mice in each group. *D*, T cell population in thymus. $CD4^-CD8^-$ DN, $CD4^+CD8^+$ DP, $CD4^+CD8^-$ SP (CD4SP), and $CD4^-CD8^+$ SP (CD8SP) cells (%) are shown as the mean ± SD of five to seven mice in each group. *E*, The differentiation of DN T cells was evaluated using CD44 and CD25 expressions. Figures are representative of five to seven mice in each group. *F*, $CD44^+CD25^-$ (DN1), $CD44^+CD25^+$ (DN2), $CD44^-CD25^+$ (DN3), and $CD44^-CD25^-$ (DN4) cells (%) are shown as the mean ± SD of five to seven mice in each group. *, $p < 0.05$; **, $p < 0.005$.

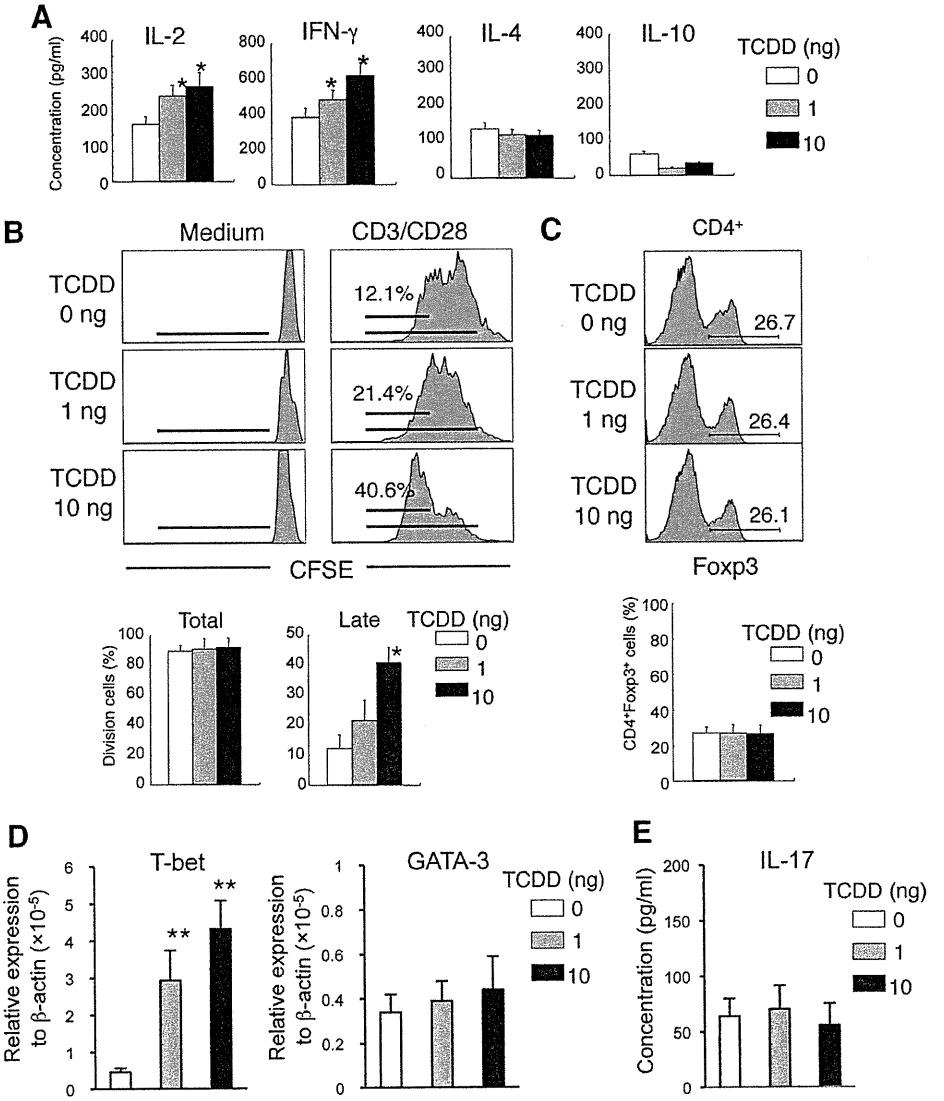

FIGURE 3. T cell functions in low-dose TCDD-treated mice. *A*, T_H1 and T_H2 type cytokine productions were analyzed by ELISA using the culture supernatants from splenic T cell-stimulated plate-coated anti-CD3 mAb for 24 h. Results are shown as mean ± SD of triplicates and representative of four to five mice in each group. *B*, Proliferative response of splenic T cell-stimulated plate-coated anti-CD3 and CD28 mAbs from TCDD-treated mice was analyzed with CFSE dilutions during 72 h. Results are representative of three to five mice in each group. *C*, $Foxp3^+CD4^+$ Treg cells in spleen from TCDD-treated mice were analyzed by flow cytometry. Results are representative of three to five mice in each group. $Foxp3^+$ cells (%) are indicated as mean ± SD of three to five mice in each group. *, $p < 0.05$. *D*, T-bet and GATA-3 mRNA expressions of spleen from TCDD-treated mice were detected by real-time PCR. Data are shown as mean ± SD of four to six mice per each group. *, $p < 0.05$; **, $p < 0.005$. *E*, IL-17 production was analyzed by ELISA using the culture supernatants from splenic T cell-stimulated plate-coated anti-CD3 mAb for 24 h. Results are shown as mean ± SD of triplicates and representative of four mice in each group.

anti-CD28 mAbs, or LPS for 72 h, cell division of $CD4^+$ or $B220^+$-gated spleen cells was analyzed by flow cytometry.

ELISA

The JS-1-, SS-A/Ro-, SS-B/La-, or ss-DNA-specific Abs of sera from mice were measured by an ELISA reader (model 680; Bio-Rad) with a spectrophotometer reading at 490 nm. Igs (IgG2a and IgG1) in sera were determined by using the mouse immunoglobulins ELISA quantitation kit (Bethyl Laboratories). For detection of IL-2, IFN-γ, IL-4, IL-10, and IL-17 in the culture supernatants from anti-CD3 mAb-stimulated splenic $CD4^+$ T cells for 24 h, ELISA were performed by using each specific Ab for the cytokines as previously described (34).

Real-time quantitative RT-PCR

Total RNA was extracted from thymus, spleen, and cultured thymocytes in NFS/*sld* mice using Isogen (Wako Pure Chemical), and reverse transcribed. Transcript levels of T-bet, GATA-3, AhR, CYP1A1, Bcl-xL, TNF-α, IFN regulatory factor (IRF)-1, GADD45, IL-1β, autoimmune regulator (AIRE), salivary protein-1, GAD67, and β-actin were performed using DNA Engine OPTICOM system (Bio-Rad) with SYBR Premix Ex Tag (Takara Shuzo). Primer sequences were as follows: T-bet: forward, 5′-CCTGTTGTGGTCCAAGTTCAAC-3′ and reverse, 5′-CACAAACAT CCTGTAATGGCTTGT-3′; GATA-3: forward, 5′-GACTTGCCAGAAAG GCAGAC-3′, and reverse, 5′-AAAGAGGTCACCACCCACAG-3′; AhR: forward, 5′-ACATAACGGACGAAATCCTGACC-3′ and reverse, 5′-TC AACTCTGCACCTTGCTTAGGA-3′; CYP1A1: forward, 5′-CCATGACC GGGAACTGTGG-3′, and reverse, 5′-TCTGGTGAGCATCCTGGACA-3′; NF-κB: forward, 5′-ATGGCAGACGATGATCCCTA-3′ and reverse, 5′-TAGGCAAGGTCAGAATGCAC-3′; Bcl-xL: forward, 5′-AGAAGA AACTGAAGCAGAG-3′, and reverse, 5′-TCCGACTCACCAATACCT G-3′; TNF-α, forward, 5′-ATGAGCACAGAAAGCATGATC-3′, and reverse, 5′-AGATGATCTGAGTGTGAGGG-3′; GADD45: forward, 5′-TG GTGACGAACCCACATTCAT-3′, and reverse, 5′-ACCCACTGATCCAT GTAGCGAC-5′; IL-1β: forward, 5′-TGATGAGAATGACCTGTTCT-3′, and reverse, 5′-CTTCTTCAAAGATGAAGGAAA-3′; AIRE: forward, 5′-AAGGGAGCCCAGGTCACTAT-3′, and reverse, 5′-ATTGAGGAGGGA CTCCAGGT-3′; salivary protein-1: forward, 5′-GGCTCTGAAACTCA GGCAGA-3′, and reverse, 5′-TGCAAACTCATCCACGTTGT-3′; GAD67: forward, 5′-TGCAACCTCCTCGAACGCGG-3′, and reverse, 5′-CCAG GATCTGCTCCAGAGAC-3′; β-actin: forward, 5′-GTGGGCCGCTCT AGGCACCA-3′ and reverse, 5′-CGGTTGGCCTTAGGGTTCAG GGGGG-3′.

NF-κB transcription activity assay

The transcriptional activity of NF-κB of the nuclear extracts from thymocytes was analyzed with NF-κB transcription factor colorimetric assay kit (Millipore). Nuclear extracts were incubated with biotinylated double-strand oligonucleotide probe containing the consensus sequence for NF-κB on a streptavidin-coated plate. Captured complexes, including active NF-κB protein, were incubated with the primary Abs for p50 and RelA and HRP-conjugated secondary Ab and tetramethylbenzidine substrate. The absorbance of the samples was measured with microplate reader at 450 nm.

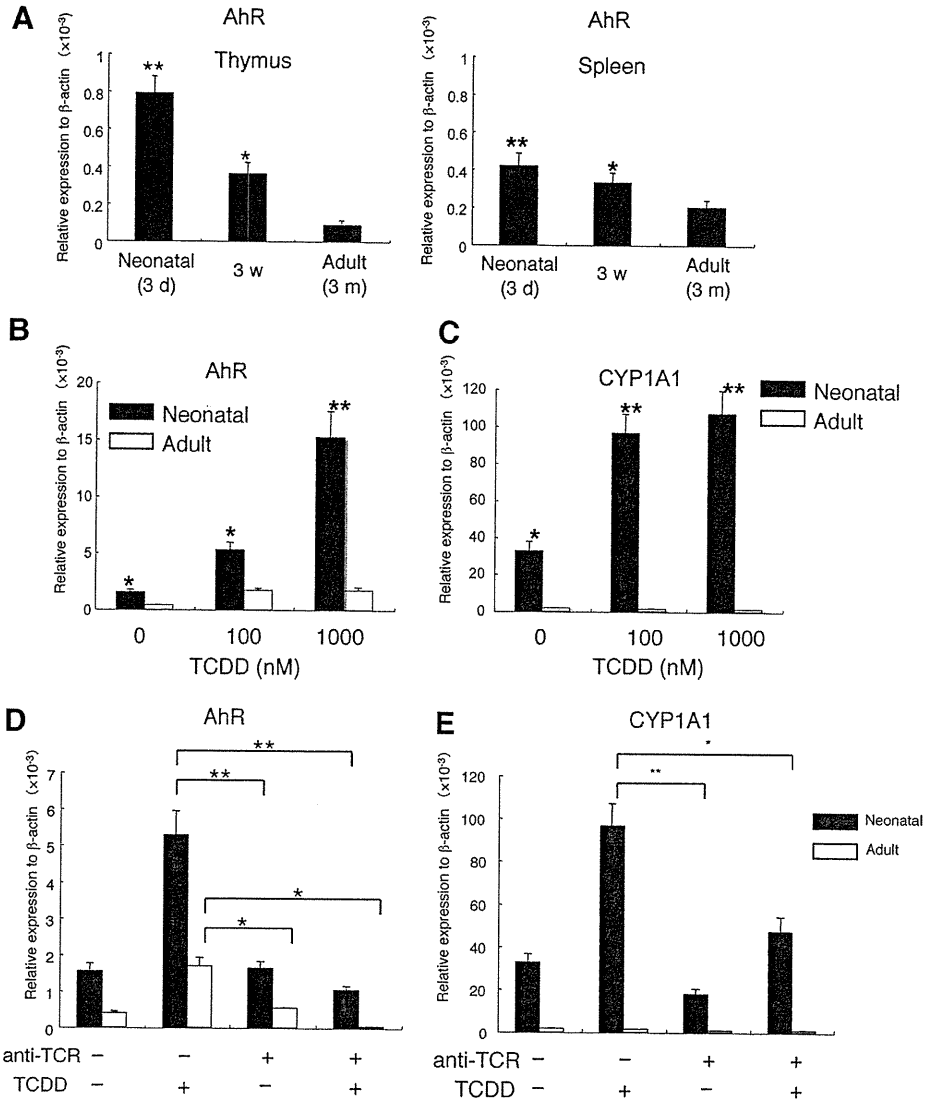

FIGURE 4. Cell signaling through AhR in thymus of NFS/*sld* mice. *A*, Expression of AhR mRNA of thymus and spleen from neonatal and adult NFS/*sld* mice was detected by quantitative RT-PCR. Relative expression to β-actin mRNA is indicated as mean ± SD of four mice in each group. *, $p < 0.05$; **, $p < 0.005$. w, Week. *B* and *C*, For 3 h in 24-well plate, 2×10^6 thymocytes of neonatal and adult NFS/*sld* mice were incubated with 0, 100, and 1000 nM TCDD. The mRNA expressions of AhR (*B*), and CYP1A1 (*C*) were analyzed by quantitative RT-PCR. *D* and *E*, The mRNA expressions of AhR (*D*) and CYP1A1 (*E*) in anti-TCR mAb-stimulated thymocytes from neonatal and adult mice with or without TCDD were detected by quantitative RT-PCR. Data are shown as mean ± SD of triplicate samples. *, $p < 0.05$; **, $p < 0.005$.

Statistical test

The Student *t* test was used for statistical analysis. Values of $p > 0.05$ were considered as significant.

Results

Induction of inflammatory lesions by neonatal administration of low-dose TCDD

To elucidate whether inflammatory lesions are induced by neonatal administration of low-dose TCDD into NFS/*sld* mice, i.p. injection of 0, 0.1, 1, and 10 ng/mouse TCDD was performed on day 0, 1, and 2 after birth. At 1, 2, and 6 mo of age, all the organs of treated mice were histopathologically analyzed. The inflammatory lesions in salivary glands of TCDD-injected mice, similar to those of thymectomized NFS/*sld* mice, were found whereas no lesion was observed in the salivary glands of vehicle-treated mice. The lesions of female mice were more severe than those of male mice (Fig. 1, *A–C*). Lymphocyte infiltration around ducts with destruction of acinar cells was observed in the TCDD-induced lesions (Fig. 1*A*). Severity of the inflammatory lesions was increased in a dose-dependent manner of TCDD (Fig. 1, *B* and *C*). In addition, more severe lesions developed with aging, and observed mainly in female mice (Fig. 1*C*). To characterize the infiltrating immune cells in the inflammatory lesions of salivary glands, the frozen sections were analyzed using the markers of T cells, B cells, and dendritic cells by immunofluorescence staining. $CD4^+$ T cells were mainly infiltrated in the inflammatory lesions of salivary glands from TCDD-treated mice, whereas a small population of $CD8^+$ T cells, B cells, and $CD11c^+$ dendritic cells were seen in the lesions (Fig. 1*D*).

In contrast, the inflammatory lesions of lung, liver, or kidney were also observed in the mice treated with TCDD (Fig. 1*E*). The incidence of the lesions is shown in Table I. At 6 mo of age, slight inflammatory lesions in the liver of 30–50% male mice by 0.1 or 1 ng of TCDD injection were observed. The inflammatory lesions of liver were found in 30–70% of male mice and ~50% of the female mice treated with 10 ng of TCDD at 6 mo of age. Also, the inflammatory lesions of lung with a small number of lymphocyte infiltrates around bronchus or blood vessels were observed in both 100% female and male mice treated with 10 ng of TCDD at 6 mo of age. In addition, the slight inflammation in the kidney from 100% male mice treated with 10 ng of TCDD was observed at 6 mo of age. As for female mice, the renal lesions were found in ~50% of the mice treated with 10 ng of TCDD at 6 mo of age. Induction of inflammatory lesions by TCDD might be dependent on the sex or the sensitivity of each organ, although its precise mechanism is unclear.

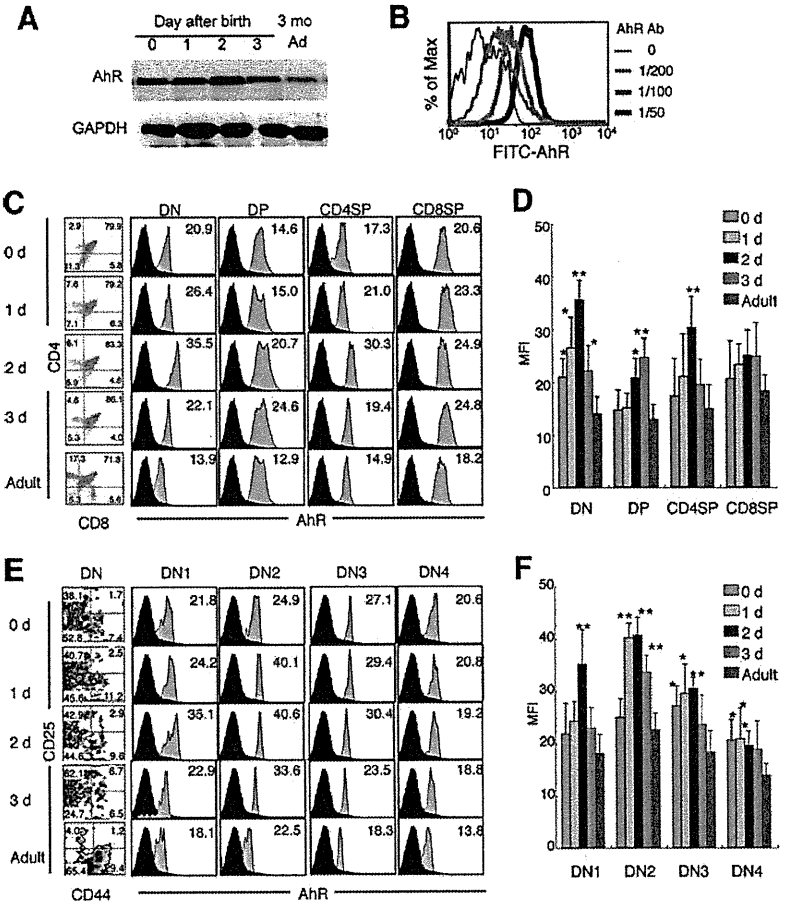

FIGURE 5. Expression of AhR in neonatal thymus. *A*, AhR protein of neonatal thymus from NFS/*sld* mice was detected by Western blotting. Result was representative of two independent experiments. GAPDH expression was used for loading control. *B*, Flow cytometric analysis of intracellular AhR expression. Thymocytes from B6 (3 mo) mice were stained with PE-Cy5.5-CD4 and PE-CD8 mAbs, fixed, washed in perm buffer, and then stained with rabbit anti-AhR Ab and FITC-conjugated anti-rabbit IgG as the second Ab. Diluted anti-AhR Ab (×200, ×100, and ×50) was used for staining. *C* and *D*, Thymocytes from neonatal (days 0, 1, 2, and 3 after birth) and adult (12 wk of age) NFS/*sld* mice were stained with PE-Cy5.5-CD4, PE-CD8, allophycocyanin-CD25, and PE-Cy7-CD44 mAbs, fixed, washed in permeabilization buffer, and then stained with rabbit anti-AhR Ab and FITC-conjugated anti-rabbit IgG as the second Ab. Intracellular AhR expressions of DN, DP, CD4SP, and CD8SP cells in neonatal and adult thymus. Figures are representative of three to four samples. Data are shown as mean ± SD of three to four samples. *E* and *F*, Intracellular AhR expression of DN cells in thymus. Data are shown as mean ± SD of mean fluorescence intensity (MFI) of three to four samples. Colored (blue or red) MFI was indicated in the figure as significantly increased. *, $p < 0.05$; **, $p < 0.005$.

Influence of in vivo low-dose TCDD injection on T cell phenotypes

To examine the influence of neonatal exposure to low-dose TCDD on T cell phenotypes, flow cytometric analysis of the expressions of surface T cell markers was performed on female mice at 6 mo of age (Fig. 2). There was no significant difference in the expression profile of CD4 and CD8 on the spleen cells by treatment of TCDD (Fig. 2*A*). A significantly increased population of memory phenotype, $CD44^{high}CD4^+$ T cell, was observed in the female mice treated with TCDD (Fig. 2*B*). As for thymic maturation, the $CD4^-CD8^-$ double-negative (DN) cells were considerably increased by treatment of 10 ng of TCDD while double-positive (DP) cells significantly decreased by 10 ng of TCDD injection. By contrast, both CD4 single-positive (SP) and CD8SP cells were significantly increased by TCDD injection (Fig. 2, *C* and *D*). Furthermore, when the increased DN cells were analyzed using differentiation markers such as CD25 and CD44, $CD44^+CD25^-$ (DN1) and $CD44^-CD25^-$ (DN4) cells were significantly reduced by in vivo treatment of 10 ng of TCDD, but significantly increased populations of $CD44^+CD25^+$ (DN2) and $CD44^-CD25^+$ (DN3) cells were observed (Fig. 2, *E* and *F*). These results suggested that neonatal exposure to TCDD might influence on thymic differentiation including negative or positive selection of T cells.

The influence of low-dose TCDD on peripheral T cell functions

To know the effect of TCDD on T cell functions in the periphery, cytokine secretions from splenic T cells activated by plate-coated anti-CD3 mAb were analyzed using the culture supernatants by ELISA. T_H1 cytokine production, including IL-2 and IFN-γ from activated T cells of TCDD-treated mice, was significantly increased compared with that of control mice (Fig. 3*A*). By contrast, there was no influence on T_H2 cytokine secretion such as IL-4 and IL-10 by in vivo TCDD injection (Fig. 3*A*). Moreover, proliferative response of splenic T cells stimulated with anti-CD3 and CD28 mAbs was analyzed using CFSE dilutions during 3 days. The cell divisions during the late stage were significantly enhanced by in vivo TCDD injection compared with those of control mice (Fig. 3*B*). In contrast, there was no difference in $Foxp3^+$ $CD25^+CD4^+$ T cells, classical Treg cells, by neonatal TCDD exposure (Fig. 3*C*). It has been known that T-bet for T_H1 and GATA-3 for T_H2 are prime candidates for key transcription factors of each cytokine production of T_H cells (35). T-bet mRNA expression of purified T cells from spleen in TCDD-treated mice was higher than that in control mice. However, there was no change of the GATA-3 mRNA expression by TCDD injection (Fig. 3*D*). In addition, to examine the role of IL-17 in the pathogenesis for TCDD-induced autoimmunity, no change was observed in IL-17 production from anti-CD3 mAb-stimulated T cells of TCDD-treated mice (Fig. 3*E*). These findings show that the neonatal exposure to low-dose TCDD influences on T cell activation or proliferation through enhanced secretion of T_H1 cytokines in the periphery.

Direct influences of TCDD on neonatal thymus

When adult NFS/*sld* mice at 2 mo of age were injected with low-dose TCDD, no inflammatory lesion in any organ was observed until 6 mo of age (our unpublished data). Neonatal exposure to low-dose TCDD may affect the induction of inflammatory lesions in salivary glands resembling the SS model. To evaluate whether

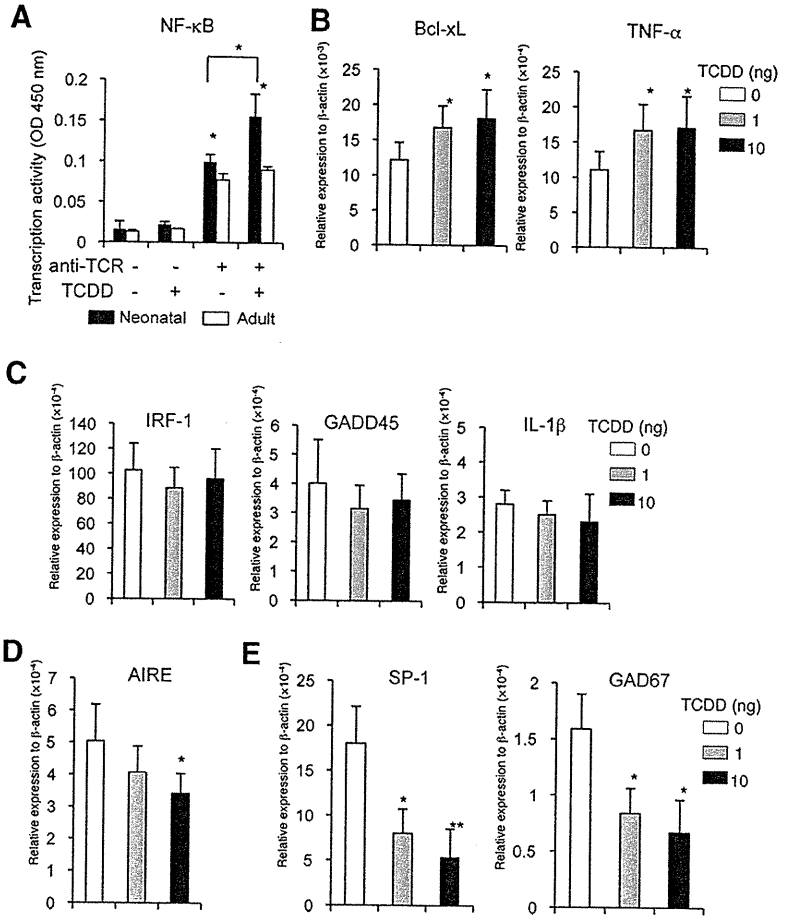

FIGURE 6. Influence of TCDD on central tolerance in thymus. *A*, Transcription activity of NF-κB in thymocytes stimulated with anti-TCR mAb in the presence or absence of TCDD was evaluated. Results are shown as mean ± SD of three samples. *, $p < 0.05$. *B* and *C*, In vivo effect of TCDD on target genes of NF-κB was evaluated to detect the mRNA expressions. The mRNA expressions of NF-κB-regulated genes in thymus tissues from TCDD-treated mice were analyzed by real time-PCR. Results are shown as mean ± SD of four to six mice per each group. *, $p < 0.05$. *D*, AIRE mRNA expression of thymus from TCDD-treated mice. *E*, The mRNA expressions of salivary protein-1 and GAD67 in thymus from TCDD-treated mice. The expressions of thymus from TCDD-treated mice were detected by real-time PCR. *, $p < 0.05$; **, $p < 0.005$.

the exposure to TCDD has much more influence on neonatal thymus compared with adult thymus, the expression of AhR was analyzed by quantitative RT-PCR. Interestingly, in contrast to adult thymus, the expression of AhR mRNA of neonatal thymus from NFS/*sld* mice was much higher (8- to 9-fold) (Fig. 4*A*). The expression was reduced with aging (~3 mo of age). The expression of AhR mRNA in neonatal spleen was higher (2-fold) than that in adult spleen (Fig. 4*A*). Next, to clarify the direct effects of TCDD on thymocytes, neonatal and adult thymocytes were incubated with 0, 100, and 1000 nM TCDD for 3 h to analyze AhR expression. More increased expression of AhR in neonatal thymocytes was observed by TCDD stimulation compared with that in adult thymocytes (Fig. 4*B*). In addition, mRNA expression of CYP1A1, one of target genes for TCDD/AhR/XRE (36), in neonatal thymocytes was much enhanced by TCDD incubation, whereas there was no change in mRNA expression of CYP1A1 in adult thymocytes by TCDD stimulation (Fig. 4*C*). In contrast, there were no significant changes in mRNA expressions of AhR and CYP1A1 of the spleen cells in the response to TCDD between neonatal and adult mice (data not shown). To understand association between TCR and TCDD signaling in thymocytes of neonatal and adult NFS/*sld* mice, plate-coated anti-TCRβ mAb was used for the stimulation of thymocytes with or without TCDD. Up-regulated mRNA expression of AhR by TCDD in both neonatal and adult thymocytes was clearly reduced by stimulation of anti-TCRβ mAb (Fig. 4*D*). In addition, TCDD-induced CYP1A1 mRNA expression in neonatal thymocytes was reduced to the level of non-stimulation by anti-TCRβ mAb (Fig. 4*E*). These findings suggest that neonatal thymocytes may be sensitive to TCDD through highly expressed AhR in NFS/*sld* mice, and that neonatal injection of TCDD might influence thymic differentiation to induce breakdown of tolerance.

Expression of AhR in neonatal thymus

To confirm the higher expression of AhR as a protein in neonatal thymus tissues of NFS/*sld* mice, Western blot analysis was performed. The highest expression of AhR was observed on day 2 after birth, and the expression on day 3 was relatively decreased. The expression in adult (3 mo of age) was lower than that of neonatal thymus (Fig. 5*A*). Next, we tried to detect the intracellular AhR expression in subpopulation of thymocytes by flow cytometric analysis. Flow cytometric analysis showed that most thymocytes clearly expressed AhR in adult (3 mo of age) C57BL/6 mice, and the fluorescence intensity of AhR expression was increased depending on the dose of anti-AhR Ab (Fig. 5*B*). When compared, the AhR expressions at each stage including DN, DP, CD4SP, and CD8SP cells in neonatal thymus of NFS/*sld* mice from day 0 to day 3 after birth with those in adult thymus (3 mo), a significantly increased AhR expression of neonatal (days 0, 1, 2, and 3) DN T cells was observed than that of adult DN cells. In particular, much more AhR expression of DN cells on day 2 was detected during neonatal stage. AhR expression of DP T cells on days 2 and 3 was significantly higher than that of adult DP cells. In contrast, although AhR expression of CD4SP cells on day 2 was significantly higher than that of adult CD4SP cells, there was no change in the expression of AhR of CD8SP cells between neonatal and adult thymus (Fig. 5, *C* and *D*). Furthermore, when the AhR expression of each differentiation stage of DN such as $CD44^+CD25^-$ (DN1), $CD44^+CD25^+$ (DN2), $CD44^-CD25^+$ (DN3), and $CD44^-CD25^-$

(DN4) cells was analyzed, AhR expressions of DN1 cells on day 2, DN2 cells on days 1, 2, and 3, DN3 cells on days 0, 1, and 2, and DN4 cells on days 0, 1, and 2 were significantly higher than those of adult DN cells (Fig. 5, *E* and *F*). Among them, the expressions of neonatal DN2 and DN3 cells were more intensive compared with those of adult thymocytes. In contrast, there was no difference in AhR expression at each stage between neonatal and adult thymocytes from normal B6 mice (data not shown). These findings suggest that AhR expression may be related with development and differentiation of T cells in neonatal thymus of NFS/*sld* mice, and that sensitivity of TCDD in neonates can be explained by the development of autoimmunity through AhR expression.

The influence of exposure to low-dose TCDD on central tolerance

Because higher AhR expression of T cells in neonatal thymus of NFS/*sld* mice was observed (Fig. 5), the cell signal pathway to regulate central tolerance in thymus via TCDD/AhR was analyzed. We focused on NF-κB, one of the responsive factors for TCDD/AhR/XRE signaling (37), which is known to be a key transcription factor for regulation of T cell differentiation, development, and activation (38). When the transcriptional activity of NF-κB in between neonatal and adult thymocytes stimulated with anti-TCR mAb in the presence of TCDD was compared, the neonatal activity was significantly increased relative to that of adult thymocytes (Fig. 6*A*). Also, the NF-κB activity of neonatal thymocytes stimulated with anti-TCR mAb was largely enhanced by the addition of TCDD, whereas the increased activity of adult thymocytes was not observed (Fig. 6*A*). Next, to understand the in vivo cell signaling through NF-κB and TCDD/AhR in thymus, the mRNA levels of NF-κB target genes were analyzed by real-time PCR using the thymus tissues from neonatal TCDD-treated mice. Among them, Bcl-xL and TNF-α mRNAs in thymus tissues from TCDD-treated mice were significantly increased in the dose-dependent manner compared with control mice (Fig. 6*B*). There were no changes to the mRNA expressions of IRF-1, GADD45, IL-1β (Fig. 6*C*), IL-6, inducible NO synthase, and Fas ligand (data not shown) which are target genes of NF-κB for controlling T cell signal.

In contrast, AIRE, an essential transcription factor for the expression of tissue-specific autoantigen in thymic epithelial cells (TECs), is well known to play a key role in T cell differentiation and development related with autoimmunity (39). When AIRE mRNA level in thymus tissues, including TECs from neonatal TCDD-treated NFS/*sld* mice, was analyzed, the expression in 10 ng of TCDD-treated mice was significantly decreased compared with that in control mice (Fig. 6*D*). Moreover, salivary protein-1 and GAD67 are known to be representative for the tissue-specific Ag in salivary gland and pancreas respectively (40). Interestingly, both salivary protein-1 and GAD67 mRNA expressions of the thymus tissues from neonatal TCDD-treated NFS/*sld* mice were significantly reduced relative to those from control mice (Fig. 6*E*). These findings show that neonatal exposure to low-dose TCDD in NFS/*sld* mice might influence the impairment of central tolerance in thymus, resulting in the induction of autoimmune disease.

The influences of low-dose TCDD exposure on B cells

The effects of neonatal exposure to low-dose TCDD on B cell phenotype and function were analyzed (Fig. 7). There was no difference in the number of $B220^+$ B cells from spleen between TCDD-treated and control mice (Fig. 7*A*). Furthermore, no change was observed in the proliferative response of splenic B cells to LPS from TCDD-treated mice compared with that from control mice (Fig. 7*B*). The serum titers of autoantibodies that are associated with SS, including anti-SSA/Ro, anti-SSB/La, and anti-ssDNA, were examined (17, 18). In this study, serum titers of anti-SSA/Ro and anti-SSB/La autoantibodies were significantly increased in TCDD-treated mice at 6 mo of age compared with those in control mice (Fig. 7*C*). It has been reported that thymectomized NFS/*sld* mice and human SS patients have high titers of serum autoantibody against α-fodrin (20, 34). The higher titers of anti-α-fodrin autoantibody in the sera from TCDD-treated mice were also detected from control mice at 6 mo of age (Fig. 7*D*). No significant change for anti-ssDNA was observed between TCDD-treated and control mice (data not shown). In addition, when the ratio of IgG2a and IgG1 that is associated with T_H1 and T_H2 or cellular and humoral immune responses was analyzed using sera from TCDD-injected mice, the ratio from TCDD-injected mice was significantly higher than that from control mice at 6 mo of age (Fig. 7*E*).

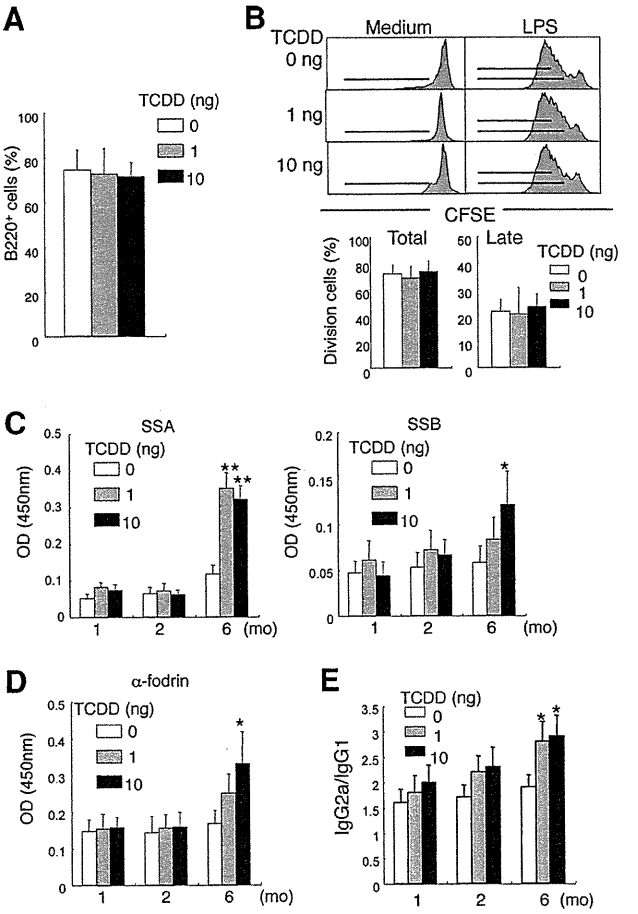

FIGURE 7. Influence on B cell functions by neonatal exposure to low-dose TCDD. *A*, $B220^+$ B cells in spleen from TCDD-treated mice at 6 mo of age were detected by flow cytometric analysis. Results are shown as mean ± SD of five to seven mice in each group. *B*, Proliferative response of splenic B cells stimulated with LPS was evaluated with CFSE dilutions during 72 h. Figures are representative of five to seven mice in each group. *C* and *D*, Serum titers of autoantibodies, including anti-SSA/Ro, anti-SSB/Lo, and anti-α-fodrin from female TCDD-treated mice from 1 to 6 mo of age were measured by ELISA. Results are shown as mean ± SD of five to seven mice in each group. *E*, Ratio of IgG2a/IgG1 in sera from TCDD-injected mice. Serum titer of IgG2a and IgG1 from TCDD-injected NFS/*sld* mice was measured by ELISA. Data are shown as mean ± SD of the ratio from five to seven mice. *, $p < 0.05$; **, $p < 0.005$.